A Model for Evaluating the Crystallinity Quality of Single Crystals Grown by the Floating Zone Technique

Benyan Xu, Zhenyou Li, Kunpeng Wang, Xuejiao Wang, Jianxiu Zhang, Lanju Liang, Longfei Li, Yanbiao Ren, Yong Liu, Meng Liu, and Dongfeng Xue**

The floating zone technique is a popular method for crystal growth of nonconventional superconductors and magnetic materials. However, the quality must be characterized with particular care with respect to their actual crystallinity since not everything grown by floating zone method is a single crystal. In this paper, the molten-zone sensitive material $LiCoPO_4$ has been grown by the floating zone method using $Co(NO_3)_2 \cdot 6H_2O$ and CoO precursors, respectively, abbreviated as LCP_N and LCP_O. The grown materials are characterized regarding their chemical composition, phase purity, crystal perfection, and orientation. In order to optimize crystal growth and quantitatively characterize its crystallinity quality, the development factor (V) has been proposed to determine the growth rate of the grains, while the orientation deviation factor (δ) for assessing the quality of the grown crystals. The development factors V for LCP_N and LCP_O are calculated to be 0.05 and 0.09, respectively, indicating that the grains of LCP_O develop faster than those of LCP_N. At the same time, the orientation deviation factor of LCP_O exceeds that of LCP_N ($\delta(LCP_O) = 2.00$, $\delta(LCP_N) = 0.77$) suggesting a higher quality for the latter. This model provides significant guidance for the evaluation of other materials grown by the floating zone method.

1. Introduction

The floating zone (FZ) technique is a powerful single crystal growth method with crucible-free, noncontamination, and fast-growth features.[1] It is capable of growing both congruently and incongruently melting materials with highest melting points. In addition, this technique allows conducting experiment at extremely high pressure up to 300 bar under a controlled gas atmosphere.[2] With great efforts been made during the past decades,[3] the FZ technique has become one of the most popular crystal growth methods for a wide range of materials, including metals, oxides, and semiconductors, as well as various nonconventional high-temperature superconductors and new magnetic materials.[4] Different from other methods such as flux growth, top seeded solution growth, and the Czochralski method, crystals grown by FZ method must be characterized with particular care with respect to their actual crystallinity. In this regard, it is worth to cite one comment from Dabkowska. Even more unsettling is the fact that reviewers of renowned journals accept works done on crystals with virtually no characterization mentioned. This creates a vicious circle, as a generation of students believes that anything grown is a single crystal.[5]

Note that many physical and physiochemical properties of a crystal material highly depend on its crystallinity and orientation. On the premise of a quality guaranty, a precise control of the crystal growing rate would be cost-effective and efficient for both research and industrial production. Under these concerns, we would like to develop an evaluation method that provides quantitative information of crystal quality and the growing capability of grains. Two indexes are proposed to help making a fair comparison of the obtained crystals and their properties, but also to be beneficial for optimizing crystal growth protocols using the FZ method.

The procedure is elucidated using olivine lithium cobalt (II) phosphate ($LiCoPO_4$) as an example. The interest in this material has been boosted by the recent discovery of unusual ferrotoroidic domains as well as by their exceptionally high applicability for electrochemical energy storage like rechargeable lithium-ion batteries.[6,7] $LiCoPO_4$ is a promising so-called 5 V-cathode material with high specific energy density up to 800 Wh kg^{-1}. Hitherto, most research works on $LiCoPO_4$ have been done on polycrystalline powder samples. However, in order to study the correlation between magnetic order and dielectric properties, and

B. Xu, K. Wang, X. Wang, J. Zhang, L. Liang, Y. Ren, Y. Liu, M. Liu
Zaozhuang University
Zaozhuang 277160, China
E-mail: webkingss@163.com
Z. Li
Helmholtz Institute Ulm (HIU) Electrochemical Energy Storage
Helmholtzstraße 11, D-89081 Ulm, Germany
L. Li
State Key Lab of Advanced Metals and Materials
University of Science and Technology Beijing
Beijing 100083, China
D. Xue
Multiscale Crystal Materials Research Center
Shenzhen Institute of Advanced Technology
Chinese Academy of Sciences, Shenzhen 518055, China
E-mail: zdfjlkj@uzz.edu.cn

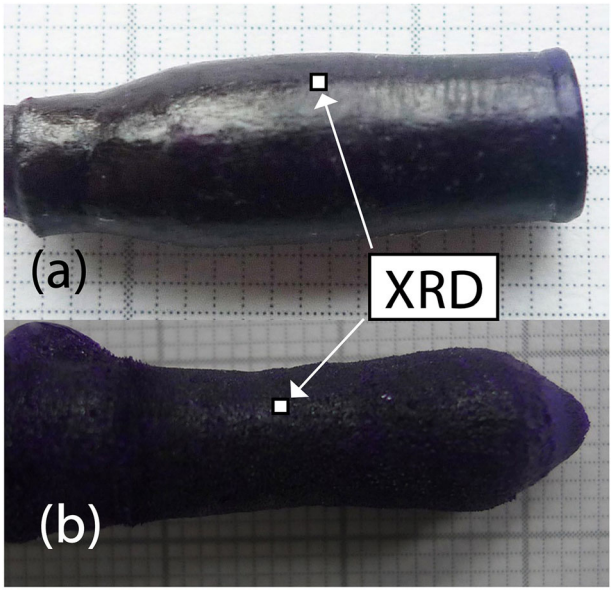

Figure 1. As-grown $LiCoPO_4$ crystals with a) $Co(NO_3)_2 \cdot 6H_2O$ and b) CoO as the starting materials.

to investigate the anisotropic electronic and ionic conductivity, large single crystals are indispensable.

In this paper, $LiCoPO_4$ single crystals have been grown by the FZ method using $Co(NO_3)_2 \cdot 6H_2O$ and CoO precursors. The corresponding crystals are abbreviated as LCP_N and LCP_O, respectively. Full characterization of the materials applying the above-mentioned method reveals information on the growth details. The results show that the grains of LCP_O develop faster than that of LCP_N while the latter is of higher semicrystalline quality. To further assess the grown crystals, two indexes are proposed: the development factor (V) to evaluate the growth rate of the grains in the crystal boule; and the orientation deviation factor (δ) for assessing the quality of the grown crystals. We hope this model would be a guideline for evaluation of the other crystal boules grown by the FZ method.

2. Results and Discussions

2.1. Crystal Growth

Figure 1 shows the as-grown rods of LCP_N and LCP_O with the sizes of Φ 6 mm × 24 mm and Φ 8 mm × 30 mm, respectively. The grown LCP_N displays purple-black color and the surface is smooth and shinning (Figure 1a). The LCP_O boule shown in Figure 1b has a purple color as well, however with a rough surface. The color of the materials is directly affected by the valence of the metal ions, indicating the LCP_O crystal mainly contains Co^{3+}-ions. Since the oxidation of Co^{2+} to Co^{3+} leads to phase separation in LCP crystals, a precise control of the sintering atmosphere, temperature, pressure, and time of the feed rod, as well as the growth atmosphere will be essential for stabilizing the Co^{2+} ions and thus obtaining a perfect single crystal. In addition, we found out that a post annealing treatment of the LCP crystal could also change its color by releasing the stress in the crystal, and adjusting the Li content and distribution.

A first assessment on the stability of the growth process can be deduced from the actual shape of the material after being molten in the image furnace. In general, the viscosity and the homogeneity of the melt in the molten zone are key factors that influence the stability of the crystal growth. They supposed to vary upon changing the precursor materials. During LCP_O growth, there was a steep gradient of the rod diameter toward the crystal seed, implying a low stability of the crystallization process. Although the homogeneity of the melt was found good during the experiment, it tends to overflow from the molten zone due to its low viscosity, which makes the control of the crystal growth with equal diameters difficult (see Figure 1b). In contrast, the LCP_N crystal could readily grow in a more stable condition, benefiting from a suitable viscosity of the melt, which makes a smoother transport of the liquid feed.

2.2. Crystal Characterization

Chemical analysis was performed on both LCP_N and LCP_O samples by means of energy-dispersive X-ray analysis. Three different spots on the cross-cut sections were selected for determination of their chemical composition. Li content cannot be analyzed by a standard EDX measurement. A typical EDX spectrum of LCP_N exhibits Co, P, O, and N peaks, in addition to the C peak stemming from the coating layer (see **Figure 2**). As shown in **Table 1**, the composition of LCP_O (23.37% P and 21.48% Co in At%) is close to the nominal $LiCoPO_4$ stoichiometry (P:Co = 1:1), which is also in the good agreement with the molar ratio of the precursors. For LCP_N, the Co/P ratio (20.97% Co and 21.16% P) matches with the nominal stoichiometry as well, even though a small amount of N impurity (4.05% in At%) was detected.

The phase purity of the grown crystals was characterized applying a grinded piece of the materials by powder XRD (see Figure 1). The resultant diffraction patterns are shown in **Figure 3**. The single-phase orthorhombic olivine-like structure was observed for both of LCP_N and LCP_O with a tiny unknown impurity peak marked as * in both of the patterns. All major peaks can be well indexed to orthorhombic $LiCoPO_4$ (PDF#32-0552).

The crystal structures of the grown crystals were refined by GSAS program according to PDF#32-0552 for $LiCoPO_4$. As an example, the fitting of LCP_N is presented in **Figure 4**, where all the major reflections are indexed with small deviation from the observed pattern. The analysis yields the lattice parameters of LCP_N $a = 10.194(0)$ Å, $b = 5.914(6)$ Å, $c = 4.693(2)$ Å, and the unit cell volume of 282.975 Å^3, and the CHI2 = 1.827 at room temperature, which are in good agreement with previously reported data.[9]

The LCP_N and LCP_O boules were longitudinal- and cross cut in order to study their defect and grain evolution during the crystal growth by polarization microscopy. **Figure 5** shows the polarized images of the longitudinal-cut sections of a) LCP_N and b) LCP_O, as well as the cross-cut sections of c) LCP_N and d) LCP_O. The white arrows indicate the growth directions. The images of the longitudinal-cuts in Figure 5a,b imply that the defects in the materials decrease when proceeding along the growth direction while in contrast the grain size increases significantly.

From Figure 5a,b we can see that the defects become less and less, and whereas the grains grow larger and larger along the

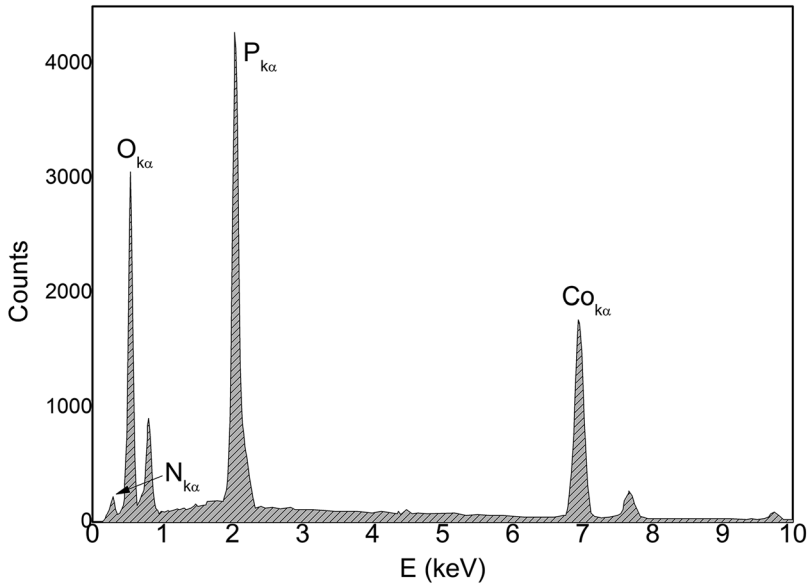

Figure 2. The EDX spectrum of LCP_N.

Table 1. The chemical composition as determined by EDX analysis on three areas on the cross-section of the LCP_N and LCP_O crystals, respectively.

		At%			
		Spot 1	Spot 2	Spot 3	Avg
LCP_N	N	3.71	4.37	4.07	4.05
	O	53.56	53.65	54.23	53.81
	P	21.25	20.71	21.54	21.16
	Co	21.48	21.27	20.17	20.97
	Sum	100	100	100	100
LCP_O	O	56.24	54.92	54.27	55.14
	P	23.04	23.44	23.63	23.37
	Co	20.72	21.63	22.10	21.48
	Sum	100	100	100	100

growth directions marked as the white arrows. Also, the grains have the tendency to coherently grow along the same crystallography direction. For convenience, we divided the longitudinal section of the crystal into four parts along the growth directions: 1) part I: the initial growth stage which shows a disorder nature, 2) R: the defect recovering stage, 3) M: the middle growth stage, and 4) E: the end growth stage. In our experiment, we set the length of R, M, and E growth zones to be equal, and furthermore, define the size factor (S) of the grains in each growth zone as

$$S = L/N \tag{1}$$

where N is the number of grains in a certain growth zone. L is the length of the growth zone. The development factor of the grains (V) is defined as the second-order derivative of a quadratic polynomial. The corresponding curve of the polynomial should pass through the three points S_R, S_M, and S_E, which are determined by the size factor of grains in R, M, and E growth zones, respectively. The V value is usually greater than zero in a normal growth experiment, otherwise the growth process is unstable or deteriorative. The larger the V value, the faster the grains grow. The expression of V can be written as

$$V = \frac{\partial^2 f(x)}{\partial x^2} \tag{2}$$

$$f(x) = a + bx + cx^2 (c \neq 0) \tag{3}$$

In our experiments, the lengths of I, R, M, and E for LCP_N are 2, 6, 6, and 6 mm, respectively. For LCP_O, the length of I, R, M, and E are 5, 4, 4, and 4 mm, respectively. For LCP_N, the number of grains among the R, M, and E parts were estimated to be 320, 95, and 32, and whereas 220, 55, and 12 for LCP_O. Then the size factors S_R, S_M, and S_E of the grains can be calculated to be 0.02, 0.06, and 0.2 for LCP_N, as well as 0.02, 0.07, and 0.3 for LCP_O, respectively. **Figure 6** shows the fitted curves of the three points S_R, S_M, and S_E, and the quadratic polynomial fitted by the least squares fitting method were given as following

$$f(x)_{LCP_N} = 0.08 - 0.11x + 0.05x^2 \tag{4}$$

$$f(x)_{LCP_O} = 0.15 - 0.22x + 0.09x^2 \tag{5}$$

The development factors of LCP_N and LCP_O grains can be calculated to be 0.05 and 0.09 indicating that the LCP_O grains grow faster than that of LCP_N, and at the same time, the defects of LCP_O recover more quickly than that of LCP_N during the crystal growth.

Whether we can successfully produce a single crystal mainly depends on whether the grains grow with highly coherent orientations or not. Here we developed a method to characterize the orientation mismatch degree of the grains during crystal growth. The orientations of the grains can be determined by the X-ray

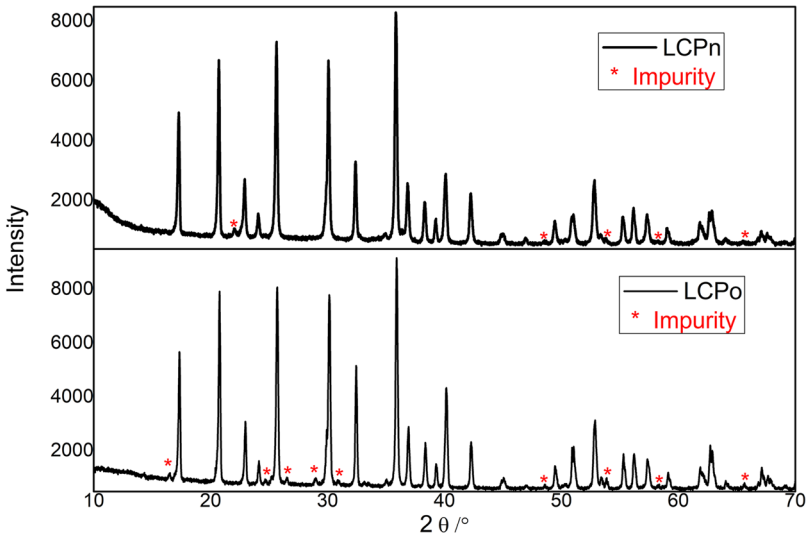

Figure 3. X-ray powder diffraction patterns for the LCP_N and LCP_O.

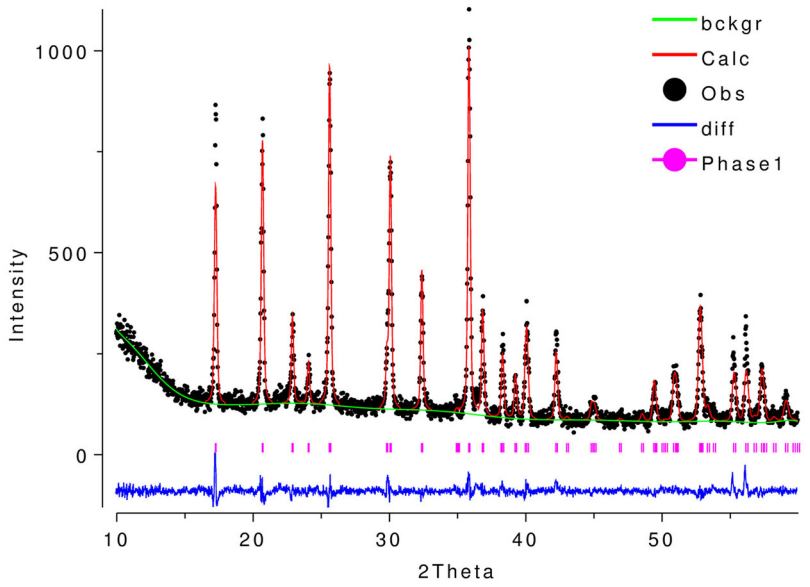

Figure 4. Results of fitting the X-ray powder diffraction data of the LCP_N: experimental (points), calculated (solid line), and difference (bottom).

Laue back scattering technique. We define the orientation deviation factor (δ) of the grains as

$$\delta = |\theta - \theta_{ref}| + |\varphi - \varphi_{ref}| \quad (6)$$

and the inclination angle (ψ) between the crystallographic planes and the Laue film as

$$\psi = (\theta, \varphi) \quad (7)$$

where θ *and* φ are the deviation angles along x *and* y axis on the Laue film, repetitively. The grain whose measurement plane has the minimum deviation degree $\zeta_{min} = (|\theta| + |\varphi|)_{min}$ to the film is taken as a reference. The inclination angle of the reference grain can be expressed as $\psi_{ref} = (\theta_{ref}, \varphi_{ref})$. The relationship of the θ, φ, Laue spot s, distance between the crystal and the film l, as well as the x- *and* y-axis of the film were shown in Figure 6b. Based on this, we can deduce that

$$\theta = \arctan(a/l) \quad (8)$$

$$\varphi = \arctan(b/l) \quad (9)$$

where a and b are the distances between the center of the film and the projection of the Laue spot s on the x and y axis of the film, respectively. In our experiments, the distance l is 4.03 cm.

Figure 5c,d shows the polarized images of the cross-cut LCP sections. Several large size grains were observed separated by the boundaries. The selected grains were marked as 1, 2, 3, and 4 on the cross-cut sections of LCP_N and LCP_O, respectively. Orientation experiments were performed on these selected grains. **Fig-**

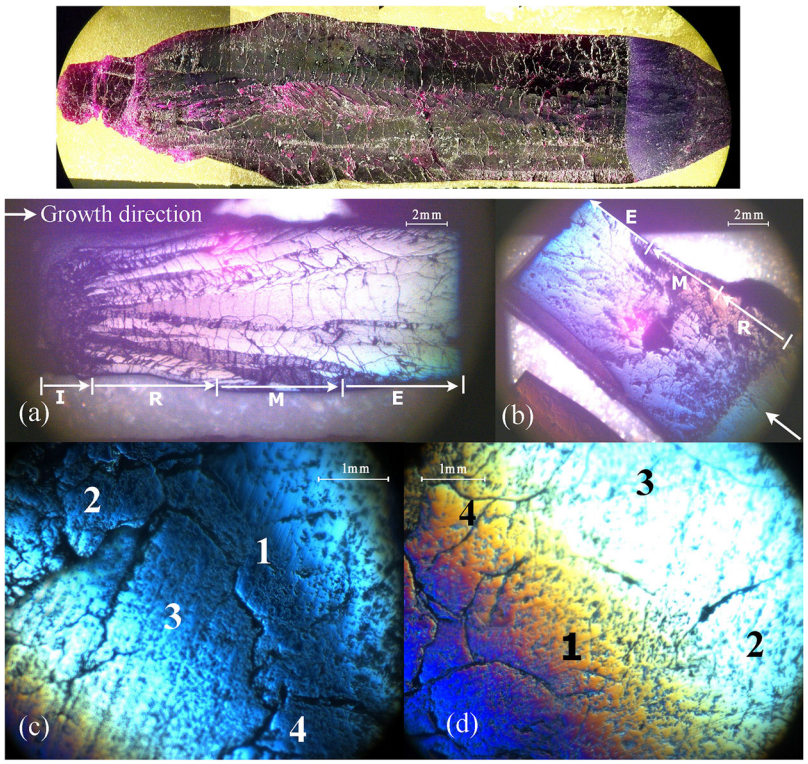

Figure 5. Polarized images of longitudinal-cut sections of a) LCP_N, and b) LCP_O, as well as the cross-cut sections of c) LCP_N, and b) LCP_O. The white arrows indicate the grown directions. The four selected grains are marked as 1, 2, 3, and 4, respectively.

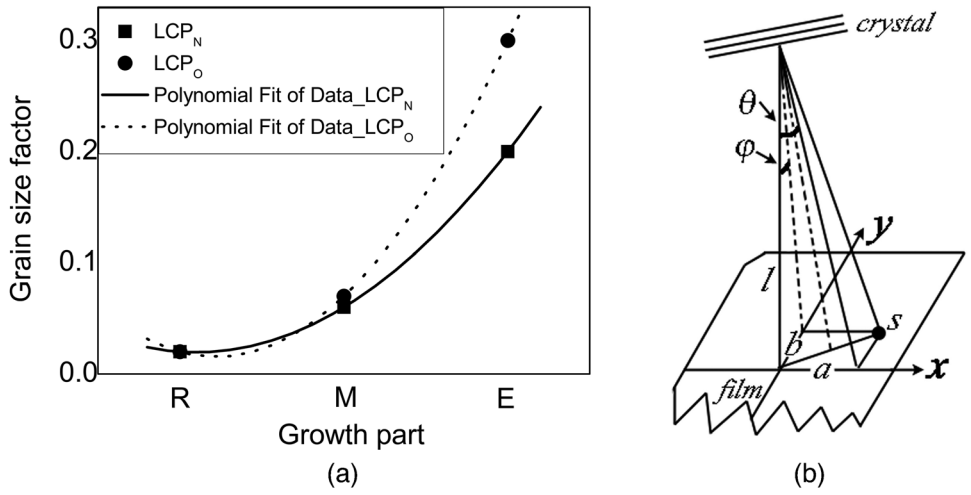

Figure 6. a) The fitted curves of the three points S_R, S_M, and S_E. b) The relationship of the θ, φ, Laue spot *s*, distance between the crystal and the film *l*, as well as the *x and* y axis of the film.

ure 7 shows the X-ray Laue back scattering images of the four selected grains on cross-cut LCP_N sections (a–d) experimental patterns, and (a′–d′) simulated patterns, as well as the four selected grains on cross-cut LCP_O sections (e–h) experimental patterns, and (e′–h′) simulated patterns.

The calculated *a*, *b*, θ, φ, and δ for the ($\bar{1}$00) Laue spots corresponding to the ($\bar{1}$00) crystallographic planes of the selected grains of LCP_N and LCP_O were listed in **Table 2**. For LCP_N, we take the grain 1 as the reference since it has the minimum deviation degree $\zeta_{min} = (|-0.0866| + |0.3886|) = 0.4752$ comparing to the film, and in the same way, we choose the grain 2 as the reference for LCP_O. From Table 2, it can be seen that the orientation deviation factor (δ) of the grains 2, 3, and 4 for LCP_N are 0.3866, 0.3705, and 0.0152, respectively, with the grain 1 as the reference. The orientation deviation factors of the grains 1, 3, and 4 for LCP_O are 1.0049, 0.5845, and 0.4078, respectively, with the grain 2 as

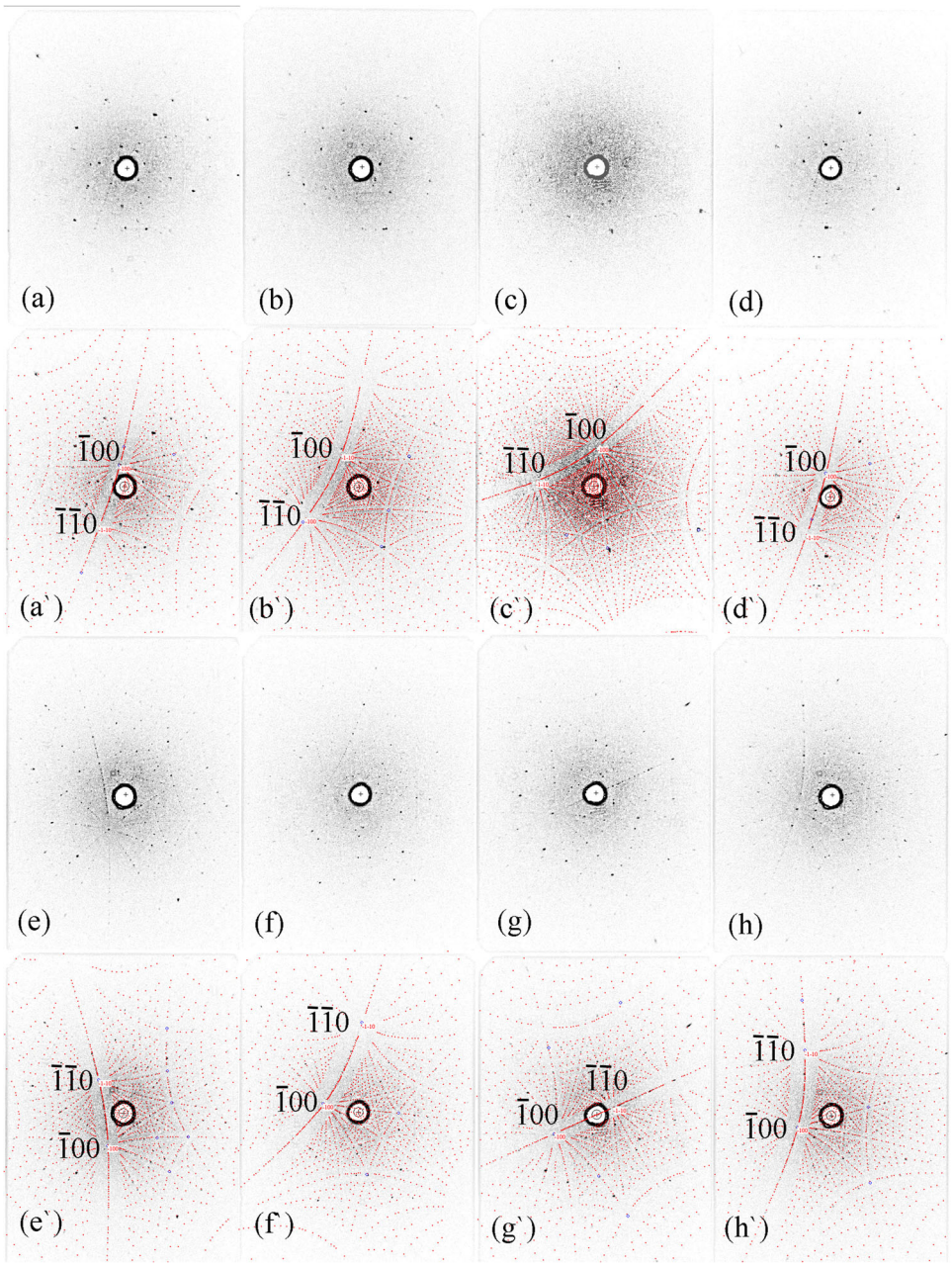

Figure 7. X-ray Laue back scattering images of the four selected grains on cross-cut LCP_N sections a–d) experimental patterns, and a′–d′) simulated patterns, as well as the four selected grains on cross-cut LCP_O sections e–h) experimental patterns, and e′–h′) simulated patterns.

the reference. The total orientation deviation factors for LCP_N and LCP_O are calculated to be 0.7723 and 1.9972, respectively, indicating that the grown LCP_N has a better quality than that of LCP_O. The larger grain mismatch of LCP_O than that of LCP_N during the crystal growth means that the single crystal or oriented grains could be easier obtained using the $Co(NO_3)_2 \bullet 6H_2O$ as the starting materials. The results agree with that the faster the growth, the worse the quality under the same growth conditions. This model has a significant guidance for evaluation of the other materials grown by the floating zone method.

3. Conclusions

$LiCoPO_4$ crystals have been grown by floating zone method with different precursor materials under 2 bar Ar atmosphere. The grown crystals were carefully characterized by polarized microscopic images, X-ray Laue back scattering technique, X-ray powder diffractions, and the EDX measurement. A quantitative method was developed by introducing two key factors, in order to characterize the growth rate and the quality of the grains. We hope to further build criteria or guidelines for evaluation

Table2. The calculated a, b, θ, φ, and δ for the ($\bar{1}$00) Laue spots corresponding to the ($\bar{1}$00) crystallographic planes of the selected grains of LCP_N and LCP_O.

Grains	a [cm]	b [cm]	θ [°]	φ [°]	δ [°]
LCP_N					
1	−0.35	1.65	−0.0866	0.3886	0
2	−1.34	2.42	−0.3210	0.5408	0.3866
3	0.27	2.79	0.0669	0.6055	0.3705
4	-0.34	1.71	−0.0842	0.4013	0.0152
LCP_O					
1	−1.19	−2.45	−0.2871	−0.5462	1.0049
2	−2.66	0.66	−0.5834	0.1623	0
3	−3.23	−1.38	−0.6756	−0.3299	0.5845
4	−2.54	−0.92	−0.5624	−0.2244	0.4078

of materials grown by the FZ method through the established method.

4. Experimental Section

Crystal Growth: Polycrystalline samples of $LiCoPO_4$ were prepared by using solid-state reaction techniques with a stoichiometric mixture of Li_2CO_3 (Chempur 99+%) and $NH_4H_2PO_4$ (Chempur 99+%) as well as either $Co(NO_3)_2{\bullet}6H_2O$ (Aldrich 99.9+%) or CoO (Aldrich 99.9+%) under Argon flowing. The chemical reactions are listed as following

$$Li_2CO_3 + 2Co(NO_3)_2 \cdot 6H_2O + 2NH_4H_2PO_4 \rightarrow 2LiCoPO_4 + CO_2\uparrow + 9H_2O\uparrow + 2NH\uparrow + 2N_2O_5\uparrow \quad (10)$$

$$Li_2CO_3 + 2CoO + 2NH_4H_2PO_4 \rightarrow 2LiCoPO_4 + CO_2\uparrow + 3H_2O\uparrow + 2NH_3\uparrow \quad (11)$$

The mixtures were grounded carefully to ensure homogeneous mixing, and then were sintered at 800 °C for 15 h. Consequentially, the products were pressed to form polycrystalline feed rods (EPSI Engineered Pressure Systems; 2000 bar) in latex tubes with a diameter of 6 mm followed by sintering again at 800 °C for 15 h.

$LiCoPO_4$ crystal growth was conducted by recrystallizing the above mentioned feed rods using a floating zone furnace with optical heating (Crystal System Incorporation, Japan). The lights of four 1000 W air-cooled xenon lamps were reflected and focused to the crystal growth chamber, which consists of a quartz tube with 2 mm wall thickness. The applied Ar pressure in the growth chamber is 2 atm. The feed rods were rotated clockwise at a rate of 20 rpm, and the seed anticlockwise 20 rpm. The growth rate was 2.5 mm h^{-1}. Two floating-zone experiments with $Co(NO_3)_2{\bullet}6H_2O$ and CoO as the starting materials were conducted, respectively.

Characterization: The elemental analysis was performed by means of a scanning electron microscope (LEO 440) with Oxford Inca X-Max 80 detector. X-ray powder diffraction (XRD) was done on a Siemens D500 in Bragg–Brentano geometry applying Cu-Kα_1 radiation (λ = 1.54056 Å) in 2θ steps of 0.02°. The XRD data were refined using the program GSAS.[8] The microstructures, the crystal perfection, and the evolution of the grains and defects were investigated on longitudinal- and cross-cut sections of both crystals by an optical microscopy in a polarization microscope (Axiovert 25) equipped with a digital camera (Zeiss). The orientation of the crystal grains was determined by the X-ray Laue back-scattering method. The growth rate of the grains was evaluated by the development factor (V). The quality of the grown crystals was evaluated by the orientation deviation factor (δ) of the grains.

Acknowledgements

B.X. and Z.L. contributed equally to this work. Supported by State Key Lab of Advanced Metals and Materials, USTB, Project No. 2021-ZD06, National Natural Science Foundation of China, grant numbers 52002350 and 51832007, and Natural Science Foundation of Shandong Province, grant number ZR2020ZD35.

Conflict of Interest

The authors declare no conflict of interest.

Data Availability Statement

Research data are not shared.

Keywords

development factor, lithium-ion batteries, orientation deviation factor, travelling-solvent floating zone

[1] W. G. Pfann, *J. Met. Trans. AIME* **1952**, *4*, 747.

[2] K. P. Wang, A. Maljuk, C. G. Blum, T. Kolb, C. Jähne, C. Neef, H.-J. Grafe, L. Giebeler, H. Wadepohl, H.-P. Meyer, S. Wurmehl, R. Klingeler, *J. Cryst. Growth* **2014**, *386*, 16.

[3] a) H. Keck, M. J. E. Golay, *Phys. Rev.* **1953**, *89*, 1297; b) M R. Null, W. W. Lozier, *Rev. Sci. Instrum.* **1958**, *29*, 163; c) L. L. Abernethy, T. H. Ramsey, J. W. Ross, *J. Appl. Phys.* **1961**, *32*, S376; d) H. C. Theuerer, US Patent, 3060123, 1962-06-26; e) T. Akashi, K. Matumi, T. Okada, T. Mizutani, *IEEE Trans. Magn.* **1969**, *5*, 285; f) I. Shindo, N. Kitamura, S. Kimura, *J. Cryst. Growth* **1979**, *46*, 307; g) A. Mühlbauer, Int. Scientific Colloq. Modell. Mater. Process., Riga **2006**.

[4] A. Lüdge, H. Riemann, M. Wünscher, G. Behr, W. Loeser, A. Muiznieks, A. Croell, *Floating Zone Crystal Growth*, in: Springer Handbook of Crystal Growth, Springer, New York **2010**.

[5] H. A. Dabkowska, A. B Dabkowski, *Springer Handbook of Crystal Growth*, Part B, Springer, New York **2010**, p. 203.

[6] A. S. Zimmermann, D. Meier, M. Fiebig, *Nat. Commun.* **2014**, *5*, 4796.

[7] a) J. M. Tarascon, M. Armand, *Nature* **2001**, *414*, 359; b) S. Y. Chung, J. T. Bloking, Y. M. Chiang, *Nat. Mater.* **2002**, *1*, 123; c) S. P. Herle, B. Ellis, N. Coombs, L. F. Nazar, *Nat. Mat.* **2004**, *3*, 147.

[8] A. C. Larson, R. B Dreele, General Structure Analysis System (GSAS), Los Alamos National Laboratory Report LAUR, **1994**, pp. 86–748.

[9] J. M. Osorio-Guillén, B. Holm, R. Ahuja, B. Johansson, *Solid State Ionics* **2004**, *167*, 221.